Mineralogical Magazine (2020), **84**, 367–375
doi:10.1180/mgm.2020.19

CAMBRIDGE UNIVERSITY PRESS

The 52nd Hallimond Lecture

Processes of metastable-mineral formation in oxidation zones and mine waste

Juraj Majzlan*
Institute of Geosciences, Friedrich-Schiller University, Burgweg 11, 07749 Jena, Germany

Abstract

Oxidation zones and mine wastes are metal-rich, near-surface environments, natural and man-made critical zones of ore deposits, respectively. They contain a number of minerals which, despite their metastability, occur consistently and in abundance. Field studies, presented as examples in this work, show that metastable minerals form not only directly from aqueous solutions, but also from more complex precursors, such as nanoparticles, gels, X-ray amorphous solids, or clusters. Initial precipitation of metastable phases and their conversion to stable phases is described by the Ostwald's step rule. Thermodynamic data show that there is a tendency, but no rule, that structurally more complex phases are also thermodynamically more stable. The Ostwald's step rule could then state that the initial metastable phases are structurally simple and easily assembled from aqueous solutions, nanoparticles, gels, disordered solids, or clusters. The structural similarity of the precursor and the forming phase is a kinetic factor favouring the crystallisation of the new phase. Calculation of saturation indices for mine drainage solutions show that they are mostly supersaturated with respect to the stable phases and the aqueous concentrations are sufficient to precipitate metastable minerals. In our fieldwork, we often encounter gelatinous substances with copper, manganese or tungsten that slowly convert to metastable oxysalt minerals. Another possibility is the crystallisation of various metastable minerals from solid, homogeneous 'resins' that are X-ray amorphous. Minerals typical for near-surface environments may be stabilised by their surface energy at high specific surface areas. For example, ferrihydrite is often described as a metastable phase but can be shown to be stable with respect to nanosised hematite.

Keywords: metastable minerals, oxidation zone, mine waste, Ostwald step rule, precursors

(Received 29 January 2020; accepted 13 March 2020; Accepted Manuscript published online: 18 March 2020; Associate Editor: Runliang Zhu)

Introduction

Oxidation zones and mine wastes are critical zones of ore deposits, either *in situ* or after human-driven re-deposition, respectively. The critical zone is a near-surface environment, a thin layer connecting atmosphere and geosphere (Küsel *et al.*, 2016). Within the critical zone, metal cycling, mineral precipitation and dissolution may be driven by inorganic processes or by organisms (Chorover *et al.*, 2007; Gadd, 2012) and can be traced by various mineralogical and geochemical methods (Blanckenburg and Schuessler, 2014; Li *et al.*, 2017). The oxidation zones and mine wastes are dynamic geochemical reactors where the primary minerals transform in contact with water, oxygen, CO_2, and biological activity to a suite of secondary phases (Williams, 1990; Lottermoser, 2010). Oxidation zones deviate much from natural, pristine and uncontaminated critical zones but they provide valuable information about metal cycling in the interface between the atmosphere and bedrock.

***Author for correspondence:** Juraj Majzlan, Email: juraj.majzlan@uni-jena.de
Cite this article: Majzlan J. (2020) Processes of metastable-mineral formation in oxidation zones and mine waste. *Mineralogical Magazine* **84**, 367–375. https://doi.org/10.1180/mgm.2020.19

In dumps, tailings and metallurgical waste, oxidation and decomposition is relatively fast and converges, in terms of mineralogy and geochemistry, with the natural oxidation zones. Many secondary minerals are metastable and convert at variable rates to the stable phases. Why and how do these metastable minerals form in the first place? Why do we find in some systems (for example, copper arsenates) so many metastable phases? The goal of this work is to contemplate on the origin of many metastable minerals in the oxidation zones and mine wastes. They serve as superb examples of the processes in the near-surface environments. Because of the elevated concentration of many metals and metalloids, they are much more amenable to many laboratory techniques with higher detection limits, including various types of microscopy as visualisation methods, for example transmission electron microscopy (e.g. Petrunic *et al.*, 2009).

Metastability and structural complexity of minerals

The relative stability or metastability of minerals seems to be associated with their structural complexity (Krivovichev, 2013), although a quantitative link is missing. It seems that more stable polymorphs are those which are more structurally complex. For

The annual Hallimond lecture is a tribute to Arthur Francis Hallimond (1890–1968) in recognition of his contribution to the science of mineralogy, particularly in the fields of ore mineralogy and instrument design (https://www.minersoc.org/hallimond-lecture.html). The 52nd Hallimond Lecture was given at the IMA meeting at Melbourne, Australia in 2018.

example, the Gibbs free energy difference between the polymorphs parabutlerite and butlerite [$Fe(SO_4)(OH)(H_2O)_2$] is 0.65 ± 0.19 kJ·mol^{-1}, with parabutlerite marginally more stable (Majzlan *et al.*, 2018a). Parabutlerite has, indeed, higher structural complexity of 33 bits/formula unit, compared to 25 bits/formula unit for butlerite. An almost linear relationship between stability and structural complexity was observed among $Cu_2(OH)_3Cl$ polymorphs botallackite, atacamite and clinoatacamite (Krivovichev *et al.*, 2017).

The relationship among chemically related phases is much more difficult to express; for example, the equilibrium between butlerite and amarantite [$Fe(SO_4)(OH)(H_2O)_3$] depends not only on the crystal structures of the participating phases but also on water activity or water vapour fugacity. Available data suggest that even in such cases, more complex phases may have greater stability (see Majzlan *et al.*, 2018a, their fig. 12) but this is not to say that exceedingly complex structures must be very stable.

The Ostwald's step rule assumes that the first phase to form is the one that requires the smallest activation energy, even if it is metastable. The rule is re-iterated by theoretical treatment of van Santen (1984) or ten Wolde and Frenkel (1999). It can be rephrased in terms of surface-energy arguments (Navrotsky, 2004), that the activation energy is proportional to the surface energy of the crystallising phase. There is a tendency, but no rule, that structurally more complex phases are more stable. If such relationships hold then the Ostwald's step rule may be expressed also in terms of a system initially precipitating simple structures that can be easily assembled from aqueous solutions, nanoparticles, gels and clusters. The simple structures are then converted to more complex and more stable ones. The structural similarity of the precursor and the forming phase is a kinetic factor that favours the crystallisation of the new phase. Metastable phases are promoted when the precursor and the new phase possess some structural similarities. This concept has been used for a long time in synthesis protocols within the so-called *chimie douce* (Figlarz, 1988; Livage, 2001).

Stabilisation of minerals by their surface energy

Even though not commonly considered, surface energy plays an important role in shifting the equilibria in near-surface systems with abundant high surface-area phases. Anderson (2005) stated that the thermodynamic equations only rarely need to consider other types of work than the mechanical work $-P\Delta V$. Yet, for finely divided and nanosised phases, the surface-work term $\gamma\Delta A$ needs to be included and considered.

The surface (or interface) energies were quantified early, for example by Enüstün and Turkevich (1959) or Schindler *et al.* (1965), among others. The data from Schindler *et al.* (1965) are displayed graphically in Fig. 1. In bulk crystals, tenorite (CuO) and water are 6 kJ·mol^{-1} more stable than spertiniite [$Cu(OH)_2$]. The slopes of the two lines in Fig. 1 are equal to the surface energies of the two cupric phases. They are a graphical representation of the increase of Gibbs free energy upon an increase of surface area. The point where these curves intersect is the free energy crossover. Beyond this point, the phase that was metastable in large, bulk crystals, becomes stable in the finely divided form. Hence, for finely divided cupric solids, spertiniite will be preferred over tenorite.

Such relationships are not limited to pairs or sets of crystalline phases. The precipitation of amorphous SiO_2 from supersaturated solutions is commonly explained by the markedly lower surface energy of SiO_2(am) than that of SiO_2(quartz) (Konhauser, 2006). The difference in the surface energies, on the order of a

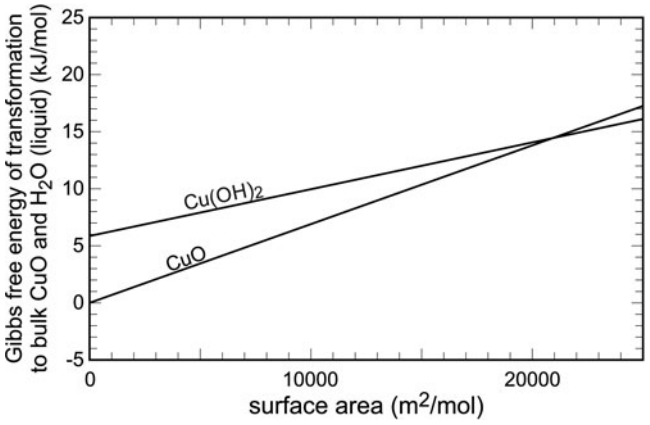

Fig. 1. Variations of Gibbs free energy with surface area in the system CuO–H_2O. Data from Schindler *et al.* (1965).

magnitude, causes precipitation of SiO_2(am) and suppression of the supersaturation with respect to SiO_2(quartz) to such a degree that quartz does not form at all.

In systems with abundant polymorphism, the relationships among the individual phases can be more complex. In the system TiO_2, there are three minerals: rutile, anatase and brookite. They are all fairly common, rutile being the one with the most occurrences. Rutile is, indeed, the most stable polymorph, but only in the bulk state. Upon gradual decrease of particle size, two crossovers are encountered (Fig. 2), both positioned at relatively low surface areas (< 4000 m^2·mol^{-1}). Hence, the TiO_2 particles do not have to attain very small sizes in order to stabilise the polymorphs anatase or brookite. The first polymorph stabilised by surface area is anatase and, at yet higher surface areas, it is brookite. The calorimetric measurements of Ranade *et al.* (2002) agree with the syntheses (e.g. Zhang and Banfield, 1998) where the finely divided initial products are made of a mixture of rutile and anatase, but coarsen progressively to rutile. They also agree with observations that leucoxene, a mineral mixture produced by weathering of Ti-bearing minerals, especially ilmenite and titanomagnetite, consists mostly of rutile and anatase, perhaps also brookite (e.g. Tyler and Marsden, 1938; Weibel, 2003), with additional goethite (α-FeOOH). Voluminous materials research literature also supports the thermodynamic considerations. Nanoparticles of rutile, anatase and brookite can be synthesised by variations of the starting chemicals and modification of the solution composition, but coarsening leads invariably to rutile (e.g. Reyes-Coronado *et al.*, 2008).

There are a number of phases in the system Fe_2O_3–H_2O, many of them with great abundance and significance for natural and man-made field systems. Extensive thermodynamic measurements (Navrotsky *et al.*, 2008) showed that hematite (α-Fe_2O_3) and goethite are the stable phases, with a finely balanced equilibrium. They both have relatively large surface energies (Fig. 3) and become metastable with respect to other Fe_2O_3 or FeOOH polymorphs at relatively low surface areas. The least stable compound in the system, the mineraloid ferrihydrite, is considered to be metastable but, in reality, seems to have such a low surface energy that it is stable, at its usual small particle size, with respect to most Fe_2O_3 or FeOOH polymorphs (Fig. 3). Within the measurement uncertainties, it is stable with respect to goethite and akaganeite at high surface areas (Fig. 3). Hiemstra (2015) showed that the surface enthalpy of ferrihydrite (0.11 J·m^{-2}) is much lower than

https://doi.org/10.1180/mgm.2020.19 Published online by Cambridge University Press

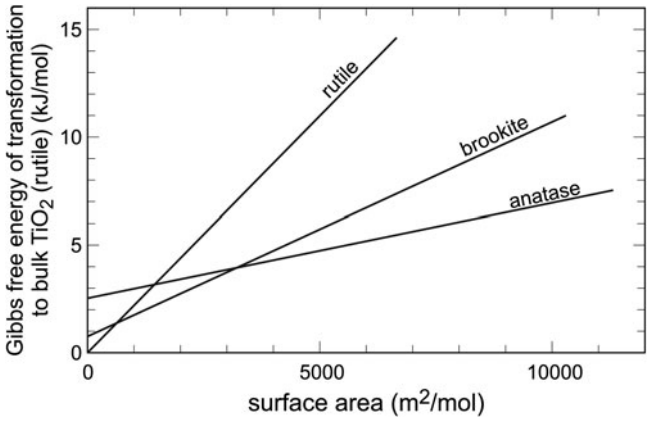

Fig. 2. Variations of Gibbs free energy with surface area in the system TiO_2. Data from Ranade *et al.* (2002).

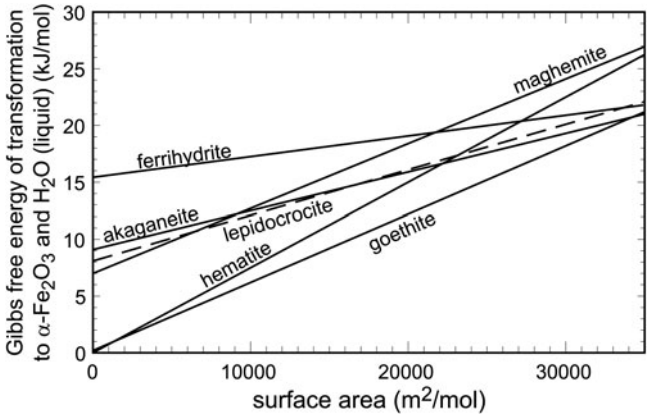

Fig. 3. Variations of Gibbs free energy with surface area in the system Fe_2O_3–H_2O. Data from Navrotsky *et al.* (2008) and Hiemstra (2015).

that of hematite (1.9 $J \cdot m^{-2}$). Using measurements (e.g. Snow *et al.*, 2013) or estimates for surface entropies, Hiemstra (2015) argued that ferrihydrite becomes thermodynamically unstable only when its particles exceed 8 nm; below this size, they appear to be stable and can persist for a long time. Ferrihydrite can be stabilised by adsorption of anions such as phosphate or arsenate. This effect can be seen in terms of kinetics, as diminution of the transformation rate (e.g. Das *et al.*, 2011) or alternatively as bulk stabilisation of a thermodynamic phase (Majzlan, 2011).

Similar measurements have been done in the system Al_2O_3–H_2O (McHale *et al.*, 1997; Majzlan *et al.*, 2000). The synthetic γ-Al_2O_3 is stabilised by its high surface area with respect to corundum (α-Al_2O_3). This conclusion agrees with observations in Nature, for example the fact that atmospheric ultrafine Al_2O_3 particles belong to the γ-Al_2O_3 phase (e.g. Jefferson, 2000). Fine-grained alumina polymorphs, especially the γ phase, find extensive use in various branches of materials science and attest their stability with respect to corundum (Levin and Brandon, 1998). The calorimetric data agree with careful solubility studies (e.g. Wesolowski and Palmer, 1994) that documented a difference in solubility product of gibbsite of ≈0.4 log units in acid-washed and untreated samples. The difference was assigned to the removal of fine particles by the acid.

The surface-area effects have been documented for manganese oxides (Birkner and Navrotsky, 2017), iron and cobalt spinels (Fe_3O_4 and Co_3O_4) and related phases (Navrotsky *et al.*, 2010) and olivine (Mg_2SiO_4) (Chen and Navrotsky, 2010). These studies bear more relevance to materials science or deep Earth, not necessarily to near-surface environments. Surface-area effects could influence some metamorphic minerals and processes (Penn *et al.*, 1999). In these cases, however, it could be assumed that the growth of the newly formed phases is relatively rapid and leaves little space for long-lasting impact of the surfaces or interfaces.

Surface-area effects *versus* metastability

The phases which are stable in their bulk form have consistently the highest surface energies. The consequence is that, if there are other phases in such systems and their metastability margin is not too large, there will be free energy crossovers. Metastable phases have lower surface energies and should be preferred during nucleation (Navrotsky, 2004). Such effects can be expected in essentially every oxide system.

Hydrated phases tend to have lower surface energies than their anhydrous counterparts. The hydrated phases will therefore be preferred and stabilised by their surface energies and could be favoured in the near-surface environments.

An important corollary of these statements is that the phases, metastable in their bulk form, will become stable in a finely divided form. Hence, in this case, metastability is suppressed and what precipitates is actually stable. The stabilisation occurs, of course, only if all participating phases have the same surface area. Otherwise, the finely divided metastable phase continues to be metastable with respect to the bulk stable phase, although it is being stabilised by its surface energy.

For simple systems other than oxides, the experimental or computational results on their surface energies are limited. Surface energy of pyrite (Raichur *et al.*, 2001; Arrouvel and Eon, 2018) is comparable to those of the iron oxides. However, a systematic view of the equilibria between the iron sulfides, including the surface-area effects, is missing. It could be only assumed that the amorphous FeS precipitates that convert to mackinawite (Michel *et al.*, 2005) and further to pyrite, are controlled by a similar driving force as the ferrihydrite–goethite or ferrihydrite–hematite transformations. Some microbial cultures have been observed to precipitate nanocrystals of sulfides that are considered to be metastable in the bulk form (Sitte *et al.*, 2013).

Surface energies of sulfates, carbonates and chlorides are one to two orders of magnitude smaller than those observed for oxides or sulfides (cf. Söhnel, 1982). In such cases, energy crossover could still be encountered but the stabilisation energy would be negligible.

Kinetic barriers for the precipitation of the stable phases

One of the simplest reasons for the formation of metastable secondary minerals is the kinetic hindrance of the stable ones (e.g. Morse and Casey, 1988; Steefel and van Cappellen, 1990). In this case, the aqueous solutions can build up the concentration of cations and anions up to that needed to precipitate metastable phases. Indeed, many stable phases (in different systems) are characterised by dense, highly polymerised structures which do not readily form from an aqueous solution. Such systems follow Ostwald's step rule, visiting a number of metastable, intermediate states before reaching the stable one.

As examples, consider the stable phases in the systems Fe_2O_3–As_2O_5–H_2O, scorodite ($FeAsO_4 \cdot 2H_2O$), CuO–As_2O_5–H_2O, olivenite [$Cu_2(OH)AsO_4$], and Fe_2O_3–Sb_2O_5, tripuhyite ($FeSbO_4$).

https://doi.org/10.1180/mgm.2020.19 Published online by Cambridge University Press

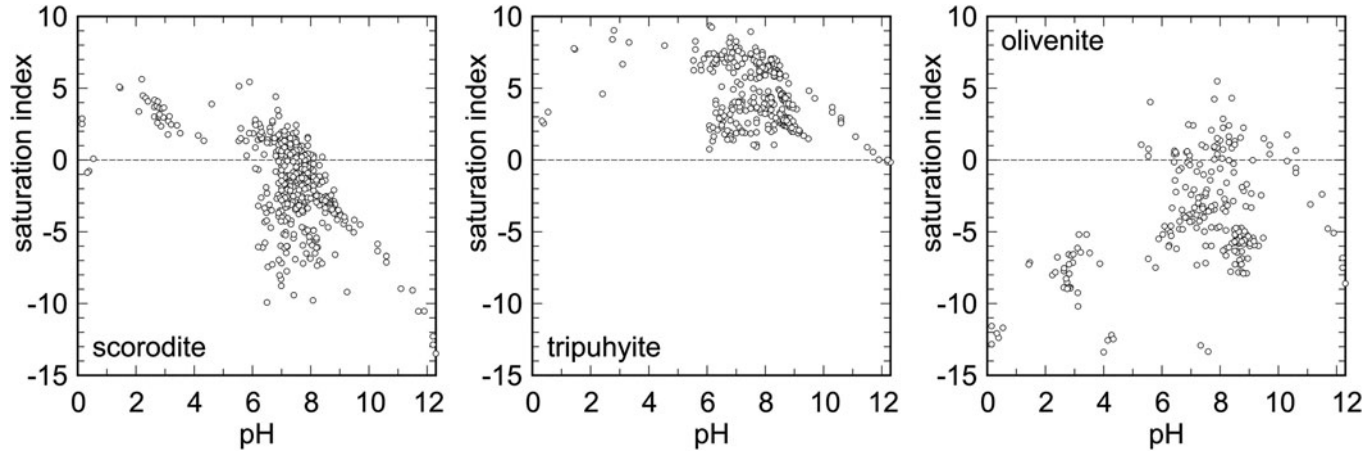

Fig. 4. Saturation indices of acidic and neutral mine drainage waters with respect to three stable minerals. For formulae and details, see text.

These systems are relevant to many sites with mine wastes. Calculation of saturation indices for these phases in more than one thousand samples of contaminated water worldwide (Fig. 4) shows that supersaturation is common. For olivenite and scorodite, the saturation indices reach values up to +6 and attest to the possibility that a less polymerised, metastable structure can form faster. Tripuhyite and the secondary antimonates represent a specific case. The aqueous solutions analysed are always supersaturated with respect to tripuhyite, considered to be the 'ultimate sink' of Sb in near-surface environments (Leverett *et al.*, 2012). Field observations show that tripuhyite forms only very slowly (Majzlan *et al.*, 2016a) and is preceded by a series of phases with greater solubility and lesser stability (e.g. Borčinová-Radková *et al.*, 2017).

Thus, supersaturation with respect to metastable phases can be reached if the nucleation and precipitation of the stable phases is too slow. Such situations may arise in portions of oxidation zones or mine wastes that are particularly rich in metals. Supersaturation of the entire volume of pore solutions in mine wastes is unlikely (e.g. Drahota *et al.*, 2012) but can be achieved in micro-environments or by processes of surface precipitation. Gräfe *et al.* (2008) observed that the surfaces of kaolinite [$Al_2Si_2O_5(OH)_4$], jarosite [$KFe_3(SO_4)_2(OH)_6$] and goethite can promote nucleation of euchroite- [$Cu_2(OH)AsO_4{\cdot}3H_2O$] and clinoclase [$Cu_3(AsO_4)(OH)_3$]-like precipitates; both of these copper arsenates are metastable with respect to olivenite. Similarly, surfaces of birnessite [$(Na,Ca,K)_xMn_2O_4{\cdot}nH_2O$] promoted crystallisation of a krautite [$Mn(AsO_3OH){\cdot}H_2O$]-like phase (Tournassat *et al.*, 2002) and the surfaces of goethite facilitated precipitation of a metastable uranyl arsenate [$UO_2(H_2AsO_4)_2{\cdot}H_2O$] (Yuan *et al.*, 2017). Jia *et al.* (2006) observed precipitation of amorphous $FeAsO_4{\cdot}nH_2O$ on the surface of ferrihydrite and ascribed the process to early surface complexation of arsenate on the surface of the iron oxide, followed by re-arrangement and initiation of surface precipitation. Such mechanisms could also operate extensively in the pristine critical zone where undersaturation with respect to many secondary oxysalts (e.g. sulfates and arsenates) is the rule but the surfaces available for adsorption and precipitation are abundant.

Nanoparticles can be stabilised through their low surface energy and possibly further growth via orientated attachment (e.g. Cölfen and Antonietti, 2005; Zhou and O'Brien, 2008; Yuwono *et al.*, 2010). Such nanoparticles can initially form by surface precipitation or by condensation of clusters. Large clusters with many metal atoms are well known for Al (Keggin cluster, Bottero *et al.*, 1987), U^{6+} (e.g. Burns and Nyman, 2018), or Nb (Friis and Casey, 2018) and could play a role in the formation of metastable minerals. Ferrihydrite is inferred to consist structurally of ferric Keggin-like clusters (Michel *et al.*, 2007). Thus, formation of nanoparticles, their growth or transformation is also linked to surface energy of the phases involved.

Crystallisation from gels

Formation of metastable oxysalts could be effortlessly ascribed to kinetic hindrance of the stable-phase crystallisation. There are plentiful examples, however, where experiments show that the kinetic barriers are small and yet, metastable phases form readily.

There are several minerals in the system $Cu_4(OH)_6SO_4$–H_2O: $Cu_4(OH)_6SO_4$ (brochantite); $Cu_4(OH)_6SO_4{\cdot}H_2O$ (posnjakite); and $Cu_4(OH)_6SO_4{\cdot}2H_2O$ (langite and wroewolfeite). There are no thermodynamic data for wroewolfeite, but among the three others, langite is the least stable, by a significant margin (17.5 $kJ{\cdot}mol^{-1}$ with respect to brochantite, Alwan and Williams, 1979; Majzlan *et al.*, 2018b). Posnjakite and brochantite can be synthesised easily and precipitate readily from aqueous solutions (e.g. Yoder *et al.*, 2007), implying that the kinetic barrier for crystallisation of the stable phases is small. The surface-energy arguments do not apply, as mentioned above, because the surface energies of such phases are similar and small. All this means that langite should not form but it does, at some sites in copious amounts as the most abundant mineral.

Investigation of the underground spaces at Ľubietová-Podlipa, Slovakia (Fig. 5, Majzlan *et al.*, 2018b), where langite currently forms, explained the basic features of this process. Langite does not crystallise directly from an aqueous solution, although it seems to be close to equilibrium with it. Instead, langite forms slowly from a thick gel that lines the entire floor of the old adit (Fig. 5). Inside the mine, the gel, ~1 cm thick, is transparent and looks like blue ice because it lies on the surface of a water stream. X-ray absorption spectroscopy indicates that the local structure of this gel is langite-like (Majzlan *et al.*, 2018b). When taken to the laboratory, this gel turns slowly to a liquid and leaves a bluish precipitate behind. Under natural laboratory conditions of steady temperature and humidity, the gel produces millimetre-sized blue langite crystals.

https://doi.org/10.1180/mgm.2020.19 Published online by Cambridge University Press

Fig. 5. Photographs from an adit in Ľubietová, Slovakia, with masses of blue gels that crystallise langite and green malachite masses. The photograph (*b*) is a detail from (*a*).

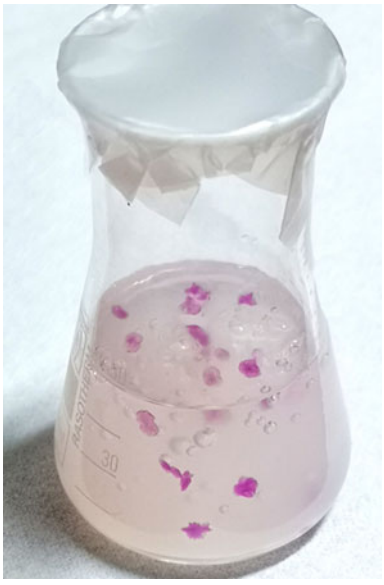

Fig. 6. Gelatinous Mn–As-bearing substance with aggregates of krautite crystals. The gel was prepared by mixing two solutions (see Buckley *et al.*, 1990) about 6 weeks before the photograph was taken.

Similar copper-rich gels were observed elsewhere in the field, although not very often. Frédéric *et al.* (2012) reported gels that precipitate copper sulfates, chlorides and carbonates in Chuquicamata, Chile. Copper-rich gels were also described from mining sites in Ireland (Moreton and Aspen, 1993) and Wyoming, USA (Williamson, 1994). A more extensive description of a 'copper-bearing silica gel' from a Tankardstown mine in Ireland (Moreton, 2007) documented its relation to langite and chrysocolla [$Cu_{2-x}Al_x(H_{2-x}Si_2O_5)(OH)_4{\cdot}nH_2O$] from this mine. Malachite [$Cu_2(CO_3)(OH)_2$] is also present, just like at the site in Ľubietová.

Synthetic copper-bearing gels were investigated early on, for example by Finch (1914) (as "jellies") with copper acetate, ammonia and manganese sulfate. Delafontaine (1896) experimented with other elements and concluded that gels can also be formed when yttrium acetate and ammonia are mixed. More recently, Henry *et al.* (1996) precipitated nanocrystalline posnjakite from copper-acetate–sulfate gels and investigated their structure.

Other secondary minerals form from such gels as well. The synthesis of krautite [$Mn(AsO_3OH){\cdot}H_2O$] commences with mixing of two solutions and the immediate formation of a thick gel (Deiss, 1914; Buckley *et al.*, 1990). With progressing time, radial aggregates of krautite crystals form from the gel (Fig. 6) and after a few weeks or months, the gel turns to liquid and crystals sink to the bottom of the flask. Higher temperatures speed the process up but the transient gel still occurs. We found that some other members of the krautite group, for example koritnigite, can be synthesised exactly in the same way. X-ray absorption experiments (Fig. 7) on the Mn–As gel and the resulting krautite crystals showed that the local structure of the gel, even a few minutes after its formation, is already krautite-like.

The existence of $WO_3{\cdot}xFe_2O_3{\cdot}nH_2O$ gels was documented by Tarassov and Tarassova (2018) and presumed by Števko *et al.* (2017). In both cases, the gels are thought to be precursors or companions to tungstite ($WO_3{\cdot}H_2O$), hydrotungstite ($WO_3{\cdot}2H_2O$) and related minerals. Wei *et al.* (2013) noted that vigorous stirring of the starting solutions "was important to suppress the formation of gelatinous, poorly crystallized arsenate phase" during the synthesis of annabergite [$Ni_3(AsO_4)_2{\cdot}8H_2O$] and erythrite [$Co_3(AsO_4)_2{\cdot}8H_2O$].

Crystallisation from X-ray amorphous solid precursors

Apart from viscous gels that tend to turn to liquid, metastable minerals can form slowly from solid, disordered precursors. An example of a site with such minerals are the medieval dumps from silver mining in Kaňk near Kutná Hora in the Czech Republic. These dumps can be divided broadly into clayey and rocky. The clayey dumps contain nodules of the mineral bukovskýite [$Fe_2(AsO_4)(SO_4)(OH){\cdot}9H_2O$], up to a size of 1 metre. The rocky dumps contain abundant kankite [$FeAsO_4{\cdot}3.5H_2O$], zýkaite [$Fe_4(AsO_4)_3(SO_4)(OH){\cdot}15H_2O$] and parascorodite [$FeAsO_4{\cdot}2H_2O$] (e.g. Ondruš *et al.*, 1999). Scorodite, the most stable phase, is uncommon.

Microscopic and analytical work (Loun, 2010; Majzlan *et al.*, 2012) showed that bukovskýite forms from solid 'gels' or 'resins' whose composition varies widely (Fig. 8). During the evolution from SiO_2–Al_2O_3 dominated compositions towards those

https://doi.org/10.1180/mgm.2020.19 Published online by Cambridge University Press

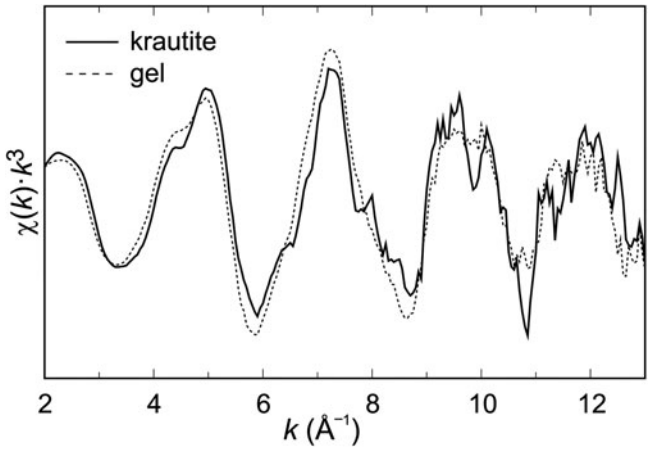

Fig. 7. Comparison of the EXAFS data for crystalline krautite and a fresh gel that turns within weeks or months into krautite (see also Fig. 6). The gel was prepared 20 minutes before the measurement, frozen at 15 K, and measured.

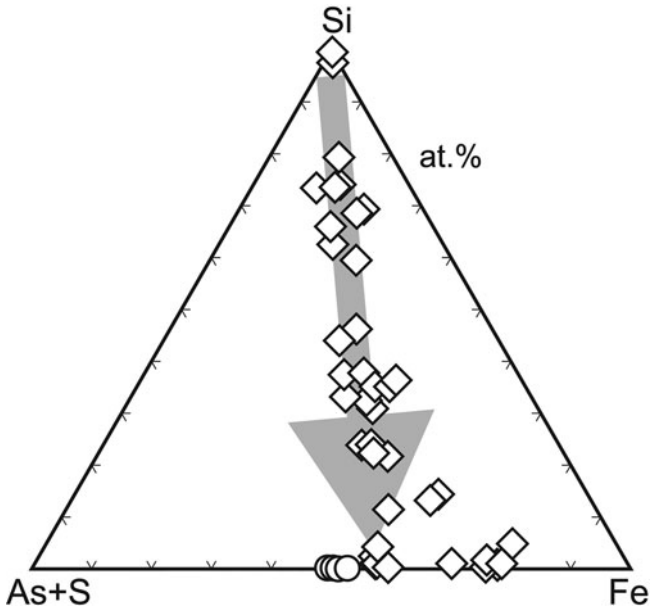

Fig. 8. Evolution of the chemical composition of X-ray amorphous solids (diamonds) that produce compact bukovskýite (circles) at Kaňk, Czech Republic. Data are electron microprobe analyses from Loun (2010) and Majzlan *et al.* (2012).

comparable to that of bukovskýite, these substances maintain approximately the Fe:As:S ratio of 2:1:1 and eventually convert to the compact crystalline bukovskýite. These gels or resins digest and incorporate the entire content of silicates and sulfides in the dumps. The end product, the bukovskýite nodules, are completely free of such minerals. We found no evidence that the crystallising nodules are able to push out or to displace mechanically the original fine-grained material of the dumps. The process is therefore of a purely chemical nature and generates large amounts of metastable secondary minerals.

Another example of such processes is the weathering of complex sulfides, such as minerals of the tetrahedrite–tennantite [$(Cu,Fe,Zn,Hg,Ag)_{12}(Sb,As)_4S_{13}$] group (Majzlan *et al.*, 2018c; Keim *et al.*, 2018). In the initial stages of such weathering, X-ray amorphous, nanocrystalline products are formed. They are unstable and slowly convert to crystalline minerals, mostly arsenates, of which some are also metastable. The transient X-ray amorphous materials are related to the antimony-bearing phases with pyrochlore structure, such as oxycalcioroméite ($Ca_2Sb_2O_6O$) or bindheimite ($Pb_2Sb_2O_6O$). Similar materials were also reported recently by Đorđević *et al.* (2019) from weathering of realgar-rich tailings which are rich in Sb but depleted in Fe. Our on-going studies indicate the presence of similar materials during weathering of Hg-tetrahedrite. In all cases, these materials are rich in As and retain large parts of this element. One of the intriguing questions is the position of arsenic in these materials because the pyrochlore structure has no tetrahedral sites available for As^{5+}. In other words, the X-ray amorphous material houses an element whose coordination preferences deviate strongly from what is available. It could be therefore assumed that the metastability of the initial X-ray amorphous material is so pronounced that its recrystallisation and re-arrangement can lead to a wide range of arsenates, including those that are metastable.

Biologically-driven disequilibria

Biologically-controlled mineralisation (see Konhauser, 2006) may generate metastable minerals that serve a specific biological purpose but such mineralisation is rarely of relevance for oxidation zones or mine wastes. The products of the biologically-induced mineralisation, either passive or facilitated (Konhauser, 2006), are much more voluminous and typical for some environments of mine wastes, for example acid mine drainage (AMD). In this case, however, the microorganisms (e.g. *Acidithiobacillus ferrooxidans*) accelerate the reactions and reduce the deviation from equilibrium; in other words, they bring such systems nearer to equilibrium. Metastable minerals, such as 'green rusts' [e.g. the minerals fougèrite, $Fe_4^{2+}Fe_2^{3+}(OH)_{12}[CO_3]\cdot 3H_2O$, trébeurdenite, $Fe_2^{2+}Fe_4^{3+}O_2(OH)_{10}CO_3\cdot 3H_2O$ and mössbauerite, $Fe_6^{3+}O_4(OH)_8[CO_3]\cdot 3H_2O$; Mills *et al.*, 2012], ferrihydrite ($FeOOH\cdot nH_2O$) or schwertmannite [$Fe_8O_8(OH)_6SO_4$], may precipitate, but their formation can be attributed to the surface-energy effects, not to the microorganisms themselves. In addition, the cells or their metabolic products may provide nucleation sites for metastable or stable minerals and lower the energetic barrier for nucleation and growth.

In some cases, however, the action of microorganisms can generate a disequilibrium situation which would be difficult to attain otherwise. In AMD water rich in Fe^{2+} and As^{3+}, *Acidithiobacillus ferrooxidans* can oxidise only Fe^{2+} but not As^{3+} (Egal *et al.*, 2009). The resulting Fe^{3+}/As^{3+} solution, in a strong redox disequilibrium, can precipitate the ferric arsenite tooeleite [$Fe_6^{3+}(As^{3+}O_3)_4(SO_4)(OH)_4\cdot 4H_2O$] (Majzlan *et al.*, 2016b). Other organisms, such as *Thiomonas* sp., oxidise both Fe^{2+} and As^{3+} and induce the formation of poorly crystalline ferric arsenates (Morin *et al.*, 2003). Another pathway to such disequilibrium situation would be dissimilatory reduction of As^{5+} in scorodite by *Shewanella* sp. (Revesz, 2015).

Conclusions

Field observations show that metastable minerals in the near-surface environments can form by precipitation from a homogeneous aqueous solution, following the Ostwald's step rule. Considering the structural relationship among polymorphs or chemically related minerals, the rule could be alternatively formulated as preferred initial formation of structurally simple phases that may transform to structurally more complex phases. An

https://doi.org/10.1180/mgm.2020.19 Published online by Cambridge University Press

implication is also that the simple structures have lower surface energies. There is no requirement of a structural relationship between the initial phase(s) and the precursor.

There are many options other than nucleation and crystallisation from homogeneous aqueous solutions, as exemplified in this work. Formation of nanoparticles, stabilisation through surface energy, and further growth via oriented attachment are possibilities often encountered in the near-surface environments. Nanoparticles could form by homogeneous or heterogeneous nucleation, surface precipitation, or by condensation of clusters. Formation of nanoparticles, their growth or transformation is also linked to surface energy of the phases involved.

In underground spaces, we commonly find gelatinous or solid X-ray amorphous substances which are apparently weathering products of primary hydrothermal minerals. The fate of such substances is not clear but they certainly bear the potential to crystallise secondary minerals, including the metastable ones. Because of their transient nature and localisation in the depth of mines or mining waste, they remain hidden and are difficult to find, characterise, and understand. Such materials can be common and constitute precursors to many metastable secondary minerals in mine waste. They are well known from synthetic chemistry but are difficult to find or easy to overlook in the field.

The metal concentrations in the oxidation zones and mine wastes is often so high that the processes of metastable-mineral formation can be observed directly. The transient substances can be sampled and inspected by techniques such as X-ray absorption spectroscopy or electron microscopy. Finally, many similar processes may operate in general in the uncontaminated critical zone but they may be more difficult to capture and describe in the field.

Acknowledgements. I am thankful to two anonymous reviewers for their constructive and detailed comments on the manuscript. Examples brought in this work are results from several projects funded by the *Deutsche Forschungsgemeinschaft*, in collaboration with many students and colleagues, especially M. Chovan, L. Jurkovič, M. Števko, and J. Plášil. I appreciate also the support and many measurement times at the ANKA synchrotron in Karlsruhe, especially to J. Göttlicher, R. Steininger, and S. Mangold, including for the yet unpublished data on krautite presented in this publication.

References

Alwan A.K. and Williams P.A. (1979) Mineral formation from aqueous solution, part II. The stability of langite, $Cu_4SO_4(OH)_6{\cdot}H_2O$. *Transition Metal Chemistry*, **4**, 319–322.

Anderson G. (2005) *Thermodynamics of Natural Systems*. 2nd Edition, Cambridge University Press.

Arrouvel C. and Eon J-G. (2018) Understanding the surfaces and crystal growth of pyrite FeS_2. *Materials Research*, **22**, 10.1590/1980-5373-mr-2017-1140

Birkner N. and Navrotsky A. (2017) Thermodynamics of manganese oxides: Sodium, potassium, and calcium birnessite and cryptomelane. *Proceedings of the National Academy of Sciences USA*, **114**, E1046–E1053.

Blanckenburg F. and Schuessler J.A. (2014) Element cycling in the critical zone as viewed by new isotope tools. *Procedia Earth and Planetary Science*, **10**, 173–178.

Borčinová-Radková A., Jamieson H. and Campbell K. (2017) Geochemistry of antimony and arsenic in freshly deposited tailings at Beaverbrook Sb mine, Newfoundland. *GAC–MAC Book of Abstracts*, p. 35.

Bottero, J.Y., Axelos, M., Tchoubar, D., Cases, J.M., Fripiat, J.J. and Fiessinger, F. (1987) Mechanism of formation of aluminum trihydroxide from keggin Al_{13} polymers. *Journal of Colloid and Interface Science*, **117**, 47–57.

Buckley A.M., Bramwell S.T. and Day P. (1990) Intercalation reactions of krautite, $HMnAsO_4{\cdot}H_2O$. *American Mineralogist*, **75**, 1140–1146.

Burns, P.C. and Nyman, M. (2018) Captivated with encapsulation: a dozen years of exploring uranium peroxide clusters. *Dalton Transactions*, **47**, 5916–5927.

Chen S. and Navrotsky A. (2010) Calorimetric study of the surface energy of forsterite. *American Mineralogist*, **95**, 112–117.

Chorover J., Kretzschmar R., Garcia-Pichel F. and Sparks D.L. (2007) Soil biogeochemical processes within the critical zone. *Elements*, **3**, 321–326.

Cölfen H. and Antonietti M. (2005) Mesocrystals: Inorganic superstructures made by highly parallel crystallization and controlled alignment. *Angewandte Chemie*, **44**, 5576–5591.

Das, S., Hendry, M.J. and Essilfie-Dughan, J. (2011) Effects of adsorbed arsenate on the rate of transformation of 2-line ferrihydrite at pH 10. *Environmental Science & Technology*, **45**, 5557–5563.

Deiss E. (1914) Ueber Herstellung und Eigenschaften der Manganoarsenatgallerte. *Kolloid-Zeitschrift*, **14**, 139–146.

Delafontaine M.M. (1896) Ueber einige kolloidale Verbindungen der seltenen Metalle. *Chemische Nachrichten*, **73**, 284.

Đorđević T., Kolitsch U., Serafimovski T., Tasev G., Tepe N., Stöger-Pollach M., Hofmann T. and Boev B. (2019) Mineralogy and weathering of realgar-rich tailings at a former As-Sb-Cr mine at Lojane, North Macedonia. *The Canadian Mineralogist*, **57**, 403–423.

Drahota P., Filippi M., Ettler V., Rohovec J., Mihaljevič M. and Šebek O. (2012) Natural attenuation of arsenic in soils near a highly contaminated medieval mine waste dump. *Science of Total Environment*, **414**, 546–555.

Egal M., Casiot C., Morin G., Parmentier M., Bruneel O., Lebrun S. and Elbaz-Poulichet F. (2009) Kinetic control on the formation of tooeleite, schwertmannite and jarosite by *Acidithiobacillus ferrooxidans* strains in an As(III)-rich acid mine water. *Chemical Geology*, **265**, 432–441.

Enüstün B.V. and Turkevich J. (1959) Solubility of fine particles of strontium sulfate. *Journal of the American Chemical Society*, **82**, 4502–4509.

Figlarz M. (1988) Chimie-douce – A new route for the preparation of new materials – Some examples. *Chemica Scripta*, **28**, 3–7.

Finch L.S. (1914) Cupric oxide jellies. *The Journal of Physical Chemistry*, **18**, 26–33.

Frédéric L., Dold B. and Fontboté L. (2012) Present copper-rich "gel" formation in the giant porphyry copper deposit of Chuquicamata (northern Chile). *Abstract Volume, 10th Swiss Geoscience Meeting*, p. 122.

Friis, H. and Casey, W.H. (2018) Niobium is highly mobile as a polyoxometalate ion during natural weathering. *The Canadian Mineralogist*, **56**, 905–912.

Gadd G.M. (2012) Microbial roles in mineral transformations and metal cycling in the Earth's critical zone. *Molecular Environmental Soil Science*, 115–165.

Gräfe M., Beattie D.A., Smith E., Skinner W.M. and Singh B. (2008) Copper and arsenate co-sorption at the mineral-water interfaces of goethite and jarosite. *Journal of Colloid and Interface Science*, **322**, 399–413.

Henry M., Bonhomme C. and Livage J. (1996) Synthesis and characterisation of copper(II) hydroxide gels. *Journal of Sol-Gel Science and Technology*, **6**, 155–167.

Hiemstra T. (2015) Formation, stability, and solubility of metal oxide nanoparticles: Surface entropy, enthalpy, and free energy of ferrihydrite. *Geochimica et Cosmochimica Acta*, **158**, 179–198.

Jia Y., Xu L., Fang Z. and Demopoulos G.P. (2006) Observation of surface precipitation of arsenate on ferrihydrite. *Environmental Science & Technology*, **40**, 3248–3253.

Jefferson D.A. (2000) The surface activity of ultrafine particles. Pp. 155–168 in: *Ultrafine Particles* (L.M. Brown, N. Collings, R.M. Harrison, A.D. Maynard and R.L. Maynard (editors). Imperial College Press.

Keim M., Staude S., Marquardt K., Bachmann K., Opitz J. and Markl G. (2018) The mineralogy of weathering products of Bi-bearing tennantite – clues for the process and the mobilisation of heavy metals and toxic elements. *Chemical Geology*, **499**, 1–25.

Konhauser K.O. (2006) *Introduction to Geomicrobiology*. Blackwell Publishing, UK.

Krivovichev, S.V. (2013) Structural complexity of minerals: information storage and processing in the mineral world. *Mineralogical Magazine*, **77**, 275–326.

Krivovichev, S.V., Hawthorne, F.C. and Williams, P.A. (2017) Structural complexity and crystallization: the Ostwald sequence of phases in the $Cu_2(OH)_3Cl$ system (botallackite – atacamite – clinoatacamite). *Structural Chemistry*, **28**, 153–159.

https://doi.org/10.1180/mgm.2020.19 Published online by Cambridge University Press

Küsel K., Totsche K.U., Trumbore S.E., Lehmann R., Steinhäuser C. and Herrmann M. (2016) How deep can surface signals be traced in the critical zone? Merging biodiversity with biogeochemistry research in a central German Muschelkalk landscape. *Frontiers in Earth Science*, **4**, 10.3389/feart.2016.00032

Leverett P., Reynolds J.K., Roper A.J. and Williams P.A. (2012) Tripuhyite and schafarzikite: two of the ultimate sinks for antimony in the natural environment. *Mineralogical Magazine*, **76**, 891–902.

Levin I. and Brandon D. (1998) Metastable alumina polymorphs: Crystal structures and transition sequences. *Journal of the American Ceramic Society*, **81**, 1995–2012.

Li L., Maher K., Navarre-Sitchler A., Druhan J., Meile C., Lawrence C., Moore J., Perdrial J., Sullivan P., Thompson A., Jin L., Bolton E.W., Brantley S.L., Dietrich W.E., Mayer K.U., Steefel C.I., Valocchi A., Zachara J., Kocar B., Mcintosh J., Bao C., Tutolo B.M., Beisman J., Kumar M. and Sonnenthal E. (2017) Expanding the role of reactive transport models in critical zone processes. *Earth-Science Reviews*, **165**, 280–301.

Livage J. (2001) Chimie douce: from shake-and-bake processing to wet chemistry. *New Journal of Chemistry*, **25**, 1.

Lottermoser B.G. (2010) *Mine Wastes. Characterization, Treatment and Environmental Impacts*. 3rd edition, Springer, 400 pp.

Loun J. (2010) *Secondary As minerals from the dumps at the locality Kaňk near Kutná Hora*. Diploma thesis, Masaryk University Brno [in Czech].

Majzlan J. (2011) Thermodynamic stabilization of hydrous ferric oxide by adsorption of phosphate and arsenate. *Environmental Science & Technology*, **45**, 4726–4732.

Majzlan J., Navrotsky A. and Casey W.H. (2000) Surface enthalpy of boehmite. *Clays and Clay Minerals*, **48**, 699–707.

Majzlan J., Lazic B., Armbruster T., Johnson M.B., White M.A., Fisher R.A., Plášil J., Loun J., Škoda R. and Novák M. (2012) Crystal structure, thermodynamic properties, and paragenesis of bukovskýite, $Fe_2(AsO_4)(SO_4)(OH)\cdot 9H_2O$. *Journal of Mineralogical and Petrological Sciences* (*Japan*), **107**, 133–148.

Majzlan J., Števko M. and Lánczos T. (2016a) Soluble secondary minerals of antimony in Pezinok and Kremnica (Slovakia) and the question of mobility or immobility of antimony in mine waters. *Environmental Chemistry*, **13**, 927–935.

Majzlan J., Dachs E., Bender Koch C., Bolanz R., Göttlicher J. and Steininger R. (2016b) Thermodynamic properties of tooeleite, $Fe_6^{3+}(As^{3+}O_3)_4(SO_4)(OH)_4\cdot 4H_2O$. *Chemie der Erde – Geochemistry*, **76**, 419–428.

Majzlan, J., Dachs, E., Benisek, A., Plášil, J. and Sejkora, J. (2018a) Thermodynamics, crystal chemistry and structural complexity of the Fe $(SO_4)(OH)(H_2O)_x$ phases: $Fe(SO_4)(OH)$, metahohmannite, butlerite, parabutlerite, amarantite, hohmannite, and fibroferrite. *European Journal of Mineralogy*, **30**, 259–275.

Majzlan J., Števko M., Chovan M., Luptáková J., Milovská S., Milovský R., Jeleň S., Sýkorová M., Pollok K., Göttlicher J. and Kupka D. (2018b) Mineralogy and geochemistry of the copper-dominated neutral mine drainage at the Cu deposit Ľubietová-Podlipa (Slovakia). *Applied Geochemistry*, **92**, 59–70.

Majzlan J., Kiefer S., Herrmann J., Števko M., Chovan M., Lánczos T., Sejkora J., Langenhorst F., Lazarov M., Gerdes A., Radková A., Jamieson H. and Milovský R. (2018c) Synergies in elemental mobility during weathering of tetrahedrite $[(Cu,Fe,Zn)_{12}(Sb,As)_4S_{13}]$: Field observations, electron microscopy, isotopes of Cu, C, O, radiometric dating, and water geochemistry. *Chemical Geology*, **488**, 1–20.

McHale J.M., Auroux A., Perrotta A.J. and Navrotsky, A. (1997) Surface energies and thermodynamic phase stability in nanocrystalline aluminas. *Science*, **277**, 788–791.

Michel F.M., Antao S.M., Chupas P.J., Lee P.L., Parise J.B. and Schoonen M.A.A. (2005) Short- to medium-range atomic order and crystallite size of the initial FeS precipitate from pair distribution function analysis. *Chemistry of Materials*, **17**, 6246–6255.

Michel, F.M., Ehm, L., Antao, S.M., Lee, P.L., Chupas, P.J., Liu, G., Strongin, D.R., Schoonen, M.A.A., Phillips, B.L. and Parise, J.B. (2007) The structure of ferrihydrite, a nanocrystalline material. *Science*, **316**, 1726–1729.

Mills, S.J., Christy, A.G., Génin, J.M., Kameda, T. and Colombo, F. (2012) Nomenclature of the hydrotalcite supergroup: natural layered double hydroxides. *Mineralogical Magazine*, **76**, 1289–1336.

Moreton S. (2007) Copper-bearing silica gel from the walls of Tankardstown mine, Co. Waterford, Ireland. *Journal of the Russell Society*, **10**, 10–17.

Moreton S. and Aspen P. (1993) Botallackite from Dooneen mine, Allihies, ounty Cork, Republic of Ireland. *Journal of the Russell Society*, **5**, 31–32.

Morin G., Juillot F., Brunneel O., Personnè J-C., Elbaz-Poulichet F., Leblanc M., Ildefonse P. and Calas G. (2003) Bacterial formation of tooeleite and mixed As(III)/V-Fe(III) gels in the Carnoules acid mine drainage, France. A XANES, XRD, and SEM study. *Environmental Science & Technology*, **37**, 1705–1712.

Morse, J.W. and Casey, W.H. (1988) Ostwald processes and mineral paragenesis in sediments. *American Journal of Science*, **288**, 537–560.

Navrotsky, A. (2004) Energetic clues to pathways to biomineralization: Precursors, clusters, and nanoparticles. *Proceedings of the National Academy of Science USA*, **101**, 12096–12101.

Navrotsky A., Mazeina L. and Majzlan J. (2008) Size-driven structural and thermodynamic complexity in iron oxides. *Science*, **319**, 1635–1638.

Navrotsky A., Ma C., Lilova K. and Birkner N. (2010) Nanophase transition metal oxides show large thermodynamically driven shifts in oxidation-reduction equilibria. *Science*, **330**, 199–201.

Ondruš P., Skála R., Viti C., Veselovský F., Novák F. and Jansa J. (1999) Parascorodite, $FeAsO_4\cdot 2H_2O$ – a new mineral from Kaňk near Kutná Hora, Czech Republic. *American Mineralogist*, **84**, 1439–1444.

Penn R.L., Banfield J.F. and Kerrick D.M. (1999) TEM investigation of Lewiston, Idaho, fibrolite: Microstructure and grain boundary energetics. *American Mineralogist*, **84**, 152–159.

Petrunic B.M., Al T.A., Weaver L. and Hall D. (2009) Identification and characterization of secondary minerals formed in tungsten mine tailings using transmission electron microscopy. *Applied Geochemistry*, **24**, 2222–2233.

Raichur A.M., Wang X.H. and Parekh B.K. (2001) Estimation of surface free energy of pyrites by contact angle measurements. *Minerals Engineering*, **14**, 65–75.

Ranade M.R., Navrotsky A., Zhang H.Z., Banfield J.F., Elder S.H., Zaban A., Borse P.H., Kulkarni S.K., Doran G.S. and Whitfield H.J. (2002) Energetics of nanocrystalline TiO_2. *Proceedings of the National Academy of Sciences USA*, **99**, 6476–6481.

Revesz E. (2015) *Solubility and stability of scorodite and adsorbed and coprecipitated arsenical 6-line ferrihydrite in the presence of Shewanella putrefaciens CN32 and Shewanella sp. ANA-3*. PhD Dissertation, University of Ottawa, Canada, 243 pp.

Reyes-Coronado D., Rogríguez-Gattorno G., Espinosa-Pesqueira M.E., Cab C., de Coss R. and Oskam G. (2008) Phase-pure TiO_2 nanoparticles: Anatase, brookite and rutile. *Nanotechnology*, **19**, 145605.

Schindler P., Althaus H., Hofer F. and Minder W. (1965) Löslichkeitsprodukte von Metalloxiden und -hydroxiden. Löslichkeitsprodukte von Zinkoxid, Kupferhydroxid und Kupferoxid in Abhängigkeit von Teilchengrösse und molarer Oberfläche. Ein Beitrag zur Thermodynamik von Grenzflächen fest-flüssig. *Helvetica Chimica Acta*, **48**, 1204–1215.

Sitte J., Pollok K., Langenhorst F. and Küsel K. (2013) Nanocrystalline nickel and cobalt sulfides formed by a heavy metal-tolerant, sulfate-reducing enrichment culture. *Geomicrobiology Journal*, **30**, 36–47.

Snow C.L., Lilova K.I., Radha A.V., Shi Q., Smith S., Navrotsky A., Boerio-Goates J. and Woodfield B.F. (2013) Heat capacity and thermodynamics of a synthetic two-line ferrihydrite, $FeOOH\cdot 0.027H_2O$. *Journal of Chemical Thermodynamics*, **58**, 307–314.

Söhnel O. (1982) Electrolyte crystal-aqueous solution interfacial tensions from crystallization data. *Journal of Crystal Growth*, **57**, 101–108.

Steefel, C.I. and van Cappellen, P. (1990) A new kinetic approach to modeling water-rock interaction: The role of nucleation, precursors, and Ostwald ripening. *Geochimica et Cosmochimica Acta*, **54**, 2657–2677.

Števko M., Sejkora J., Malíková R., Ozdín D., Gargulák M. and Mikuš T. (2017) Supergene minerals from quartz vein with Mo-W mineralization near Ochtiná, Spišsko-gemerské rudohorie Mts. (Slovak Republic). *Bulletin Mineralogie Petrologie*, **25**, 43–54 [in Slovak].

Tarassov M.P. and Tarassova E.D. (2018) Structural and chemical evolution of mineral forms of tungsten in the oxidation zone of the Grantcharitza deposit (Western Rhodopes, Bulgaria). *Bulgarian Chemical Communications*, **50**, 270–280.

ten Wolde, P.R. and Frenkel, D. (1999) Homogeneous nucleation and the Ostwald step rule. *Physical Chemistry Chemical Physics*, **1**, 2191–2196.

https://doi.org/10.1180/mgm.2020.19 Published online by Cambridge University Press

Tournassat C., Charlet L., Bosbach D. and Manceau A. (2002) Arsenic(III) oxidation by birnessite and precipitation of manganese(II) arsenate. *Environmental Science & Technology*, **36**, 493–500.

Tyler S.A. and Marsden R.W. (1938) The nature of leucoxene. *Journal of Sedimentary Petrology*, **8**, 55–58.

van Santen, R.A. (1984) The Ostwald step rule. *Journal of Physical Chemistry*, **88**, 5768–5769.

Wei C., Zhu Y., Zhang X., Wang X. and Liu J. (2013) Dissolution and solubility of the erythrite/annabergite solid solution $[(Co_xNi_{1-x})_3(AsO_4)_2{\cdot}8H_2O]$ at 25°C. *Asian Journal of Chemistry*, **25**, 7687–7696.

Weibel R. (2003) Alteration of detrital Fe-Ti oxides in Miocene fluvial deposits, central Jutland, Denmark. *Bulletin of the Geological Society of Denmark*, **50**, 171–183.

Wesolowski D.J. and Palmer D.A. (1994) Aluminum speciation and equilibria in aqueous solution: V. Gibbsite solubility at 50°C and pH 3–9 in 0.1 molal NaCl solutions (a general model for aluminum speciation; analytical methods). *Geochimica et Cosmochimica Acta*, **58**, 2947–2969.

Williams P.A. (1990) *Oxide Zone Geochemistry*. Ellis Horwood Series in Organic Chemistry, 556 pp.

Williamson M.A. (1994) Precipitation and solubility of chrysocolla in near-neutral pH mine drainage solutions, south-central Wyoming. *Geological Society of America, Abstracts*, A353.

Yoder C.H., Agee T.M., Ginion K.E., Hofmann A.E., Ewanichak J.E., Schaeffer Jr. C.D., Carroll M.J., Schaeffer R.W. and McCaffrey P.F. (2007) The relative stabilities of the copper hydroxyl sulphates. *Mineralogical Magazine*, **71**, 571–577.

Yuan F., Cai Y.W., Yang S.T., Liu Z.Y., Chen L.H., Lang Y., Wang X.K. and Wang S. (2017) Simultaneous sequestration of uranyl and arsenate at the goethite/water interface. *Journal of Radioanalytical and Nuclear Chemistry*, **311**, 815–831.

Yuwono V.M., Burrows N.D., Soltis J.A. and Penn R.L. (2010) Oriented aggregation: Formation and transformation of mesocrystal intermediates revealed. *Journal of the American Chemical Society*, **132**, 2163–2165.

Zhang H.Z. and Banfield J.F. (1998) Thermodynamic analysis of phase stability of nanocrystalline titania. *Journal of Materials Chemistry*, **8**, 2073–2076.

Zhou L. and O'Brien P. (2008) Mesocrystals: A new class of solid materials. *Small*, **4**, 1566–1574.

https://doi.org/10.1180/mgm.2020.19 Published online by Cambridge University Press